

Synergy effect of dually superposed orbital angular momentum states in atmospheric turbulence

Tao Zhang¹, Yi-Dong Liu¹, Jiandong Wang¹, Pusheng Liu¹, and Yuanjie Yang²

¹School of Physical Electronics, University of Electronic Science and Technology of China, Chengdu 610054, People's Republic of China

²School of Astronautics and Aeronautics, University of Electronic Science and Technology of China, Chengdu 611731, People's Republic of China

Abstract—We corroborate that a synergy effect may emerge when the dually superposed orbital angular momentum (OAM) states with two adjacent OAM numbers pass through weak fluctuation regime of the atmospheric turbulence. We show that this novel effect closely depends on the transition probabilities between this two OAM eigenstates for superposition. While such probabilities become larger, the synergy effect becomes more obvious. Our examples show that the synergy effect enables OAM states to better resist phase fluctuation caused by the atmospheric turbulence.

Index Terms—atmospheric turbulence, orbital angular momentum, synergy effect.

I. INTRODUCTION

Recently, orbital angular momentum (OAM) based optical communications in classical and quantum domains were widely studied, principally because it can offer considerable number of channels multiplexed for information transmission [1]–[7]. Photons carrying OAM can be employed in quantum key distribution [2], quantum secure direct communication [3] and quantum teleportation [4]. The OAM of single photon, however, is vulnerable to random phase aberrations. In particular, OAM scattering arises while a twisted light propagates in the atmospheric turbulence [8]–[11]. Paterson firstly proposed an OAM probability distribution model to describe the OAM scattering of single photons in Kolmogorov turbulence [8]. Now it is known that the Kolmogorov model failed to predict the performance of light propagating in high altitude [12], and increasing studies were carried out based on non-Kolmogorov turbulence, which is applicable on a wider scale. The OAM detection probabilities respectively for several kinds of OAM modes based on non-Kolmogorov model were calculated by expressing each mode function as a superposition of spiral harmonics [9], [10], [13]. More recently, the effects of low-order Zernike turbulence aberrations on OAM of single photons were studied in detail, which showed that turbulence z -tilt aberration is the main reason for OAM crosstalk [14].

A superposition of two OAM eigenstates, or dually superposed OAM states (DSOS) in context, can construct a two-dimensional subspace geometrically described by an OAM

Bloch sphere [15], [16]. Generally, a DSOS on the Bloch sphere can be expressed as the form $|\xi\rangle = \cos(\beta/2)|n\rangle + e^{i\theta}\sin(\beta/2)|m\rangle$, where $|n\rangle$ and $|m\rangle$ denote the OAM eigenstates with OAM numbers n and m respectively. For the angles β and θ , there are $0 \leq \beta \leq \pi$ and $0 \leq \theta < 2\pi$ respectively. In this work, we approximately estimate the detection probability of DSOS in non-Kolmogorov turbulence and discuss the effects of β and θ on the detection probability. We use the term “synergy effect”, which comes from Hermann Haken’s conception [17], to describe a new phenomenon we find. Here, the term particularly means the fact that detection probability of DSOS (see Eq. (1)) is greater than those of the two OAM eigenstates for superposition.

II. THEORY

We consider at first a monochromatic and fully coherent twisted beam propagating along z axis in free space. In cylindrical coordinates, the transverse spatial wave function of DSOS constructed by two Laguerre Gaussian (LG) modes is written as

$$\xi_{p_0}(r, \varphi, z) = \cos\left(\frac{\beta}{2}\right) u_{p_0,n}^{\text{LG}}(r, \varphi, z) + e^{i\theta} \sin\left(\frac{\beta}{2}\right) u_{p_0,m}^{\text{LG}}(r, \varphi, z), \quad (1)$$

where n and m are OAM numbers of initial DSOS, p_0 is the radial index of initial DSOS, and z is the propagation distance. Angle β dominates the weights of two modes, and $\xi_{p_0}(r, \varphi, z)$ reduces to a wave function of OAM eigenstate when $\beta = 0$ or π . Angle θ is the relative phase between two modes. $u_{p,l}^{\text{LG}}(r, \varphi, z)$ denotes the normalized LG mode function at z plane [11]

$$\begin{aligned} u_{p,l}^{\text{LG}}(r, \varphi, z) = & \sqrt{\frac{2p!}{\pi(p+|l|)!}} \frac{1}{\omega(z)} \left[\frac{\sqrt{2}r}{\omega(z)} \right]^{|l|} L_p^{|l|} \left[\frac{2r^2}{\omega^2(z)} \right] \\ & \times \exp \left[-\frac{r^2}{\omega^2(z)} - \frac{ikr^2z}{2(z^2 + z_r^2)} \right] \\ & \times \exp \left[i(2p + |l| + 1)\tan^{-1} \left(\frac{z}{z_r} \right) \right] \\ & \times \exp(-il\varphi), \end{aligned}$$

where $z_r = \pi\omega_0^2/\lambda$ is the Rayleigh range with ω_0 the waist radius and λ the wavelength. $k = 2\pi/\lambda$ is the wave

This work is supported by the National Natural Science Foundation of China under Grant nos. 60908034, 61205122 and 11474048, and Fundamental Research Funds for the Central Universities under grant nos. ZYGX2013J052 and ZYGX2015J042. Corresponding author: Yi-Dong Liu(liuyd@uestc.edu.cn)

number. $\omega(z) = \omega_0 \sqrt{1 + (z/z_r)^2}$ is the beam radius at z . p and l are the radial index and the OAM number, respectively. $L_p^l(\cdot)$ denotes the generalized Laguerre polynomial. Another transverse spatial wave function $\zeta_{p_0}(r, \varphi, z)$ being orthogonal to $\xi_{p_0}(r, \varphi, z)$ in the same subspace can be expressed as $\zeta_{p_0}(r, \varphi, z) = \sin(\beta/2)u_{p_0,n}^{\text{LG}}(r, \varphi, z) - e^{i\theta} \cos(\beta/2)u_{p_0,m}^{\text{LG}}(r, \varphi, z)$. For convenience, we assume that the initial DSOS send at $z = 0$ plane, where the radii of two LG modes are the same as ω_0 .

We restrict ourselves to the weak fluctuation regime, in which the intensity fluctuation is very small and negligible. The complex amplitude of this distorted mode at z plane reads [9], [10], [14]

$$\phi(r, \varphi, z) = \xi_{p_0}(r, \varphi, z) \exp[i\chi(r, \varphi, z)], \quad (2)$$

where $\chi(r, \varphi, z)$ corresponds to the phase fluctuation. Because an arbitrary amplitude profile can be expanded into LG modes [18], $\phi(r, \varphi, z)$ here can be expressed as

$$\begin{aligned} \phi(r, \varphi, z) &= \sum_p \sum_l A_p^l(z) u_{p,l}^{\text{LG}}(r, \varphi, z) \\ &= \sum_p B_p(z) \xi_p(r, \varphi, z) + \sum_p C_p(z) \zeta_p(r, \varphi, z) \\ &+ \sum_p \sum_{l \neq n, m} A_p^l(z) u_{p,l}^{\text{LG}}(r, \varphi, z), \end{aligned} \quad (3)$$

where p and l are the radial index and OAM number of received LG mode, respectively. $A_p^l(z)$ is the expansion coefficient. In addition, the coefficients $B_p(z)$ and $C_p(z)$ in Eq. (3) can be expressed as

$$B_p(z) = \cos(\beta/2)A_p^{l=n}(z) + \sin(\beta/2)A_p^{l=m}(z)e^{-i\theta}$$

and

$$C_p(z) = \sin(\beta/2)A_p^{l=n}(z) - \cos(\beta/2)A_p^{l=m}(z)e^{-i\theta}.$$

Because $\{u_{p,l}^{\text{LG}}(r, \varphi, z)|_{l \neq n, m}, \xi_p(r, \varphi, z), \zeta_p(r, \varphi, z)\}_{p \in \mathbb{N}}$ is a set of complete and orthogonal basis for an arbitrary amplitude $\phi(r, \varphi, z)$, the coefficient $B_p(z)$ is obtained as

$$B_p(z) = \iint \phi(r, \varphi, z) \cdot \xi_p^*(r, \varphi, z) r dr d\varphi. \quad (4)$$

We are interested in the statistic characteristic of detection probability since phase fluctuation caused by the atmosphere turbulence is random. For the sake of simplicity and without loss of generality, we assume that the receiver aperture is infinite and there is no energy loss in atmospheric turbulence. The detection probability of initial DSOS is evaluated as

$$P(\xi|\xi, p_0) = \sum_p \langle |B_p(z)|^2 \rangle \equiv \sum_p P(\xi, p|\xi, p_0), \quad (5)$$

where $\langle \cdot \rangle$ denotes the ensemble average. Here $P(\xi|\xi, p_0)$ denotes the detection probability of received state $|\xi\rangle$ meanwhile the transmitted state is $|\xi, p_0\rangle$. The p order part of $P(\xi|\xi, p_0)$ in non-Kolmogorov turbulence can be expressed as

$$\begin{aligned} P(\xi, p|\xi, p_0) &= \iiint \xi_{p_0}(r_1, \varphi_1, z) \xi_{p_0}^*(r_2, \varphi_2, z) \\ &\times \langle \exp[i\chi(r_1, \varphi_1, z) - \chi(r_2, \varphi_2, z)] \rangle \\ &\times \xi_p^*(r_1, \varphi_1, z) \xi_p(r_2, \varphi_2, z) r_1 r_2 dr_1 dr_2 d\varphi_1 d\varphi_2, \end{aligned} \quad (6)$$

where the ensemble average in right hand of Eq. (6) reads [19]

$$\begin{aligned} &\langle \exp[i\chi(r_1, \varphi_1, z) - \chi(r_2, \varphi_2, z)] \rangle \\ &= \exp \left[-\frac{r_1^2 + r_2^2 - 2r_1 r_2 \cos(\varphi_1 - \varphi_2)}{\rho_0^2} \right]. \end{aligned} \quad (7)$$

In Eq. (7), ρ_0 is the spatial coherence radius of a spherical wave propagating in non-Kolmogorov turbulence [20]

$$\rho_0 = \left[\frac{8}{\alpha - 2} \Gamma \left(\frac{2}{\alpha - 2} \right) \right]^{\frac{1}{2}} \left[\frac{2(\alpha - 1) \Gamma(\frac{3-\alpha}{2})}{\sqrt{\pi} \Gamma(\frac{2-\alpha}{2}) k^2 C_n^2 z} \right]^{\frac{1}{\alpha-2}}, \quad (8)$$

where k is the wave number. C_n^2 is the refractive-index structure constant, and α is the non-Kolmogorov turbulence parameter where $3 < \alpha < 4$. $\Gamma(\cdot)$ is the Gamma function. In our calculation, we find that the relative phase θ has no impact on $P(\xi, p|\xi, p_0)$. Therefore, we focus on the relation between the detection probability $P(\xi|\xi, p_0)$ and the weight factor β in the following.

III. NUMERICAL CALCULATION AND ANALYSIS

In order to estimate $P(\xi|\xi, p_0)$, at first we investigate $P(\xi, p|\xi, p_0)$ with small radial index p , as shown in Fig. 1. The detection probabilities of received $|\xi, p\rangle$ with $p = 0, 1$ and 2 are between 1% ~ 100%, between 0.01% ~ 1%, and below 0.01%, respectively. This shows that the radial mode scattering caused by the atmospheric turbulence arises on DSOS as well as on OAM eigenstates [21]. From previous work, we know that an OAM superposed state can be measured experimentally [22]–[24], and a lower radial OAM mode is detected more easily than a higher one in a finite receiving aperture [24]. For this reason and for the case that the received state almost falls apart into $|\xi, p = 0\rangle$ and $|\xi, p = 1\rangle$, it is acceptable to omit the higher radial order parts and make an approximate estimation as $P(\xi|\xi, p_0) \approx P(\xi, p = 0|\xi, p_0) + P(\xi, p = 1|\xi, p_0)$. As $\beta = 0$ or π , $P(\xi|\xi, p_0)$ is written as $P(n|n, p_0)$ or $P(m|m, p_0)$ respectively.

For simplicity, in all figures we use the term “peak” to describe a curve whose middle part is higher than two ends.

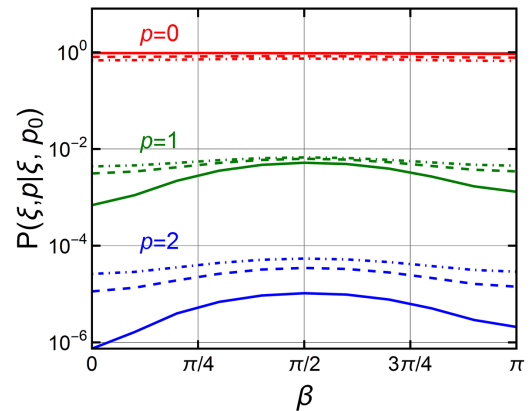


Fig. 1. The p order part of $P(\xi|\xi, p_0)$ versus β with $p=0, 1$ and 2 where $n = 0, m = 1$ (solid), $n = 5, m = 6$ (dashed), $n = 10, m = 11$ (dot-dashed). Besides, $p_0 = 0$, $\lambda = 1550\text{nm}$, $\omega_0 = 0.03\text{m}$, $z = 3000\text{m}$, $C_n^2 = 10^{-15}\text{m}^{3-\alpha}$ and $\alpha = 3.67$, respectively.

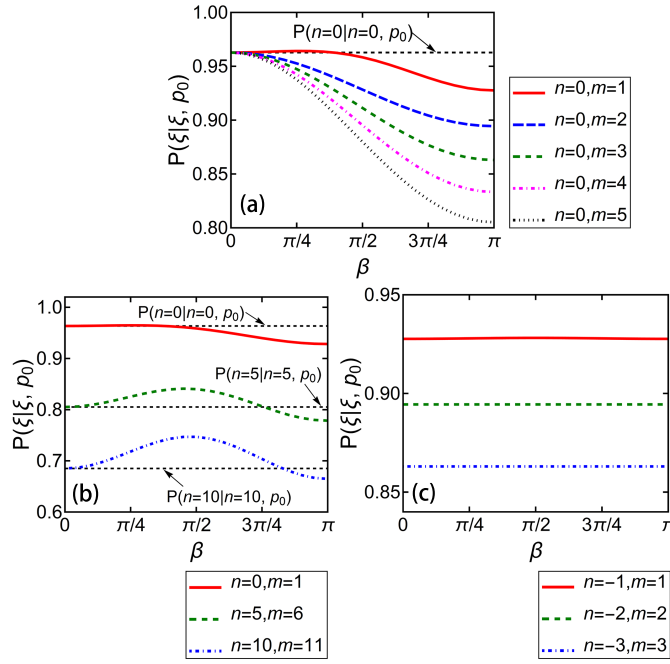


Fig. 2. (a) $P(\xi|\xi, p_0)$ versus β with $\Delta l = |n - m| = 1, 2, 3, 4$ and 5 . (b) $P(\xi|\xi, p_0)$ versus β with $\Delta l = |n - m| = 1$. (c) $P(\xi|\xi, p_0)$ versus β with $n = -m = -1, -2$ and -3 . In (a)-(c), $p_0 = 0$, $\lambda = 1550\text{nm}$, $\omega_0 = 0.03\text{m}$, $z = 3000\text{m}$, $C_n^2 = 10^{-15}\text{m}^{3-\alpha}$ and $\alpha = 3.67$, respectively.

In Fig. 2(a), $P(\xi|\xi, p_0)$ against β is plotted with different values of $\Delta l = |n - m|$. A tiny peak on the probability curve for $\Delta l = 1$ appears above the horizontal line denoted by $P(n|n, p_0)$, but no obvious peak appears for $\Delta l = 2, 3, 4, 5$. Subsequently, several cases are considered in Fig. 2(b) for $\Delta l = 1$. In Fig. 2(b), this peak always exists and becomes more obvious as n and m become larger. This peak is also above the horizontal line denoted by $P(m|m, p_0)$, because $P(n|n, p_0)$ is larger than $P(m|m, p_0)$ where $|n| < |m|$. Besides, we observe that the peak becomes more symmetrical about $\beta = \pi/2$ while the OAM numbers of DSOS become larger. In Fig. 2(c), we show some more common cases where n is contrary to m . However, there is no visible peak on the probability curve for each $n = -m$.

Figures 2(a)-2(c) show that a peak appears distinctly on the DSOS with a couple of adjacent OAM numbers, or named adjacent dually superposed OAM states (ADSOS), rather than other kinds of DSOS. The main reason for its appearance is analyzed next. $P(\xi, p|\xi, p_0)$ can be expressed as such form

$$P(\xi, p|\xi, p_0) = F_{p_0}^p + R_{p_0}^p, \quad (9)$$

where $R_{p_0}^p = \cos^2(\beta/2) \sin^2(\beta/2) [P(n, p|m, p_0) + P(m, p|n, p_0)]$, and the definition of term $F_{p_0}^p$ can be found in APPENDIX section. In order to facilitate the analysis, the radial index of initial DSOS p_0 is taken as 0. Here $P(\xi|\xi, p_0 = 0)$ can be obtained by $F + R$, where there are estimation $F \approx F_0^0 + F_0^1$ and $R \approx R_0^0 + R_0^1$. It is easy to know that the curve of term R against β shows a peak, of which the convex degree is controlled by the sum $P(n|m, p_0 = 0) + P(m|n, p_0 = 0)$. $P(n|m, p_0 = 0)$ and $P(m|n, p_0 = 0)$ are probabilities of $|m\rangle$ and $|n\rangle$ transforming

to each other in the atmospheric turbulence respectively, which have been investigated deeply in previous work [8], [9].

In Fig. 3, we plot F and R against β with $\Delta l = 1, 2, 3$ respectively. For each value of Δl , there is no visible peak on the curve of F , while curve of R shows a symmetrical profile with central peak. This fact means that if the peak on R is not pronounced enough, the detection probability of DSOS will not show any peaks because $P(\xi|\xi, p_0 = 0) = F + R$. The curve of F is more declining as Δl becomes larger. Accordingly, to form a peak on the detection probability curve, the lower limit of sum $P(n|m, p_0 = 0) + P(m|n, p_0 = 0)$ should increase as Δl increases. In addition, the peak on R

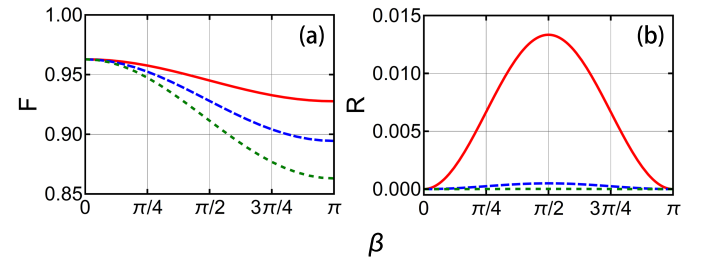


Fig. 3. The terms (a) F and (b) R against β with $n = 0, m = 1$ (red solid line), $n = 0, m = 2$ (blue long dashed line), and $n = 0, m = 3$ (green short dashed line). In (a)-(b), $C_n^2 = 10^{-15}\text{m}^{3-\alpha}$, $\alpha = 3.67$, $z = 3000\text{m}$, $\lambda = 1550\text{nm}$, $p_0 = 0$ and $\omega_0 = 0.03\text{m}$, respectively.

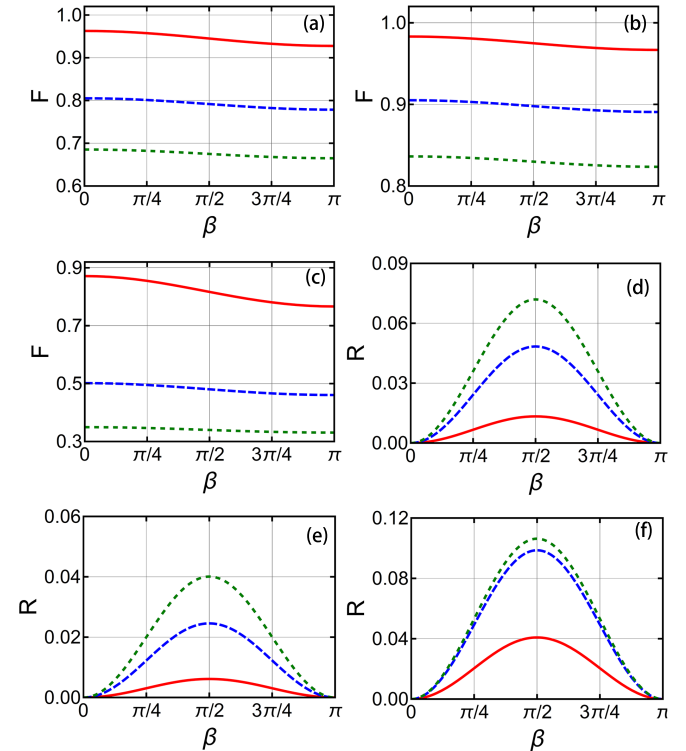


Fig. 4. F and R against β with (a) and (d): $C_n^2 = 10^{-15}\text{m}^{3-\alpha}$, $\alpha = 3.67$. (b) and (e): $C_n^2 = 5 \times 10^{-16}\text{m}^{3-\alpha}$, $\alpha = 3.67$. (c) and (f): $C_n^2 = 10^{-15}\text{m}^{3-\alpha}$, $\alpha = 3.95$. In (a)-(f), $n = 0, m = 1$ (red solid line), $n = 5, m = 6$ (blue long dashed line), and $n = 10, m = 11$ (green short dashed line). In addition, $z = 3000\text{m}$, $\lambda = 1550\text{nm}$, $p_0 = 0$ and $\omega_0 = 0.03\text{m}$, respectively.

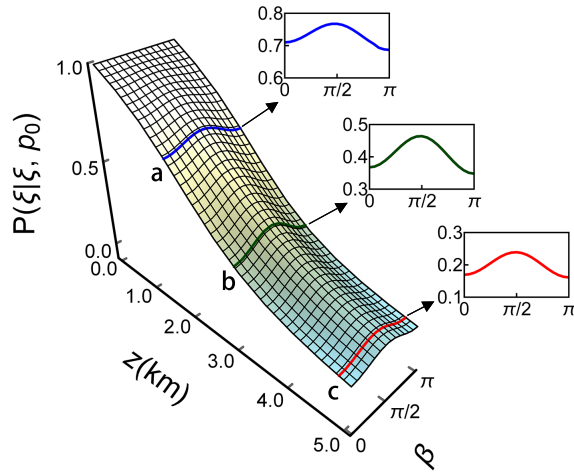


Fig. 5. Evolution of the peak on $P(\xi|\xi, p_0)$ in propagation process where $C_n^2 = 10^{-15} \text{m}^{3-\alpha}$ and $\alpha = 3.95$. In addition, $n = 10$, $m = 11$, $\lambda = 1550 \text{nm}$, $p_0 = 0$ and $\omega_0 = 0.03 \text{m}$, respectively.

becomes more obvious as Δl becomes smaller owing to the OAM spreading property in weak fluctuation regime of the atmospheric turbulence. Because of small $P(n|m, p_0 = 0) + P(m|n, p_0 = 0)$, the peaks on R for $\Delta l = 2, 3$ are not obvious. Therefore, the detection probabilities of DSOSs with $\Delta l = 2, 3$ don't show any peaks (see Fig. 2 (a)).

To exemplify the universality of our analysis, we consider F and R of several ADSOSs against β in different turbulent environments, as shown in Fig. 4. In Figs. 4 (a)-(c), we observe that the term F doesn't show obvious peaks. Moreover, as n and m become larger, the curves of F become flatter. In Figs. 4 (d)-(f), the symmetrical peaks emerging on R become more obvious as n and m become larger, thereby giving a more pronounced peak on detection probability of DSOS (see Fig. 2 (b)). Definitely, if the peak on detection probability of DSOS arises, we consider that the two parts of DSOS jointly generate a *synergy effect*.

To see how the atmospheric turbulence affects the peak on $P(\xi|\xi, p_0)$ in propagation, we consider an example illustrated in Fig. 5. We observe that the peak is enhanced at a modest distance, and weakened as z increases or decreases from that position. For example, in Fig. 5 the peak at b is more obvious than those at a and c. Following the analysis above, we can give an explanation for this phenomenon. When z is very short or very long, $P(n = 5|m = 6, p_0 = 0)$ and $P(m = 6|n = 5, p_0 = 0)$ are small because of too weak or too strong phase fluctuation [8], and thus the peak is not obvious. When z is moderate, $P(n = 5|m = 6, p_0 = 0)$ and $P(m = 6|n = 5, p_0 = 0)$ is large enough, thereby leading to a pronounced peak.

IV. CONCLUSION

In summary, we have revealed the synergy effect on DSOS in non-Kolmogorov turbulence and further analyzed the reason. Besides LG mode, other kinds of OAM modes can also be adopted to analyze this effect. The synergy effect arises obviously on DSOS if its two OAM numbers are adjacent to each other, and closely depends on the transition probabilities between the two OAM eigenstates for superposition.

Concretely, if such probabilities are small, the synergy effect is weak or even disappear. In addition, there are two important conclusions. Firstly, the synergy effect can only be fully demonstrated at a moderate transmission distance. Secondly, the relative phase of DSOS has no impact on the OAM detection probability if only phase fluctuation is considered. Further investigation with regard to the property of high-dimensional OAM superposition states in atmospheric turbulence might be enlightened by the synergy effect.

APPENDIX

In this section, we give the deduction process of Eq. (9). At first we suppose $a = \cos(\beta/2)$, $b = \sin(\beta/2)$, $u_{j,l}^{LG}(r, \varphi, z) = LG_j^l(r, z) \exp(i l \varphi) / \sqrt{2\pi}$ where $l = n, m$ and $j = p, p_0$. Firstly, we denote that

$$s_h^{i_1, i_2, i_3, i_4} = [LG_p^{i_1}(r_1, z)]^* LG_{p_0}^{i_2}(r_2, z) \times [LG_{p_0}^{i_3}(r_2, z)]^* LG_p^{i_4}(r_1, z) \times I_h\left(\frac{2r_1 r_2}{\rho_0^2}\right) \exp\left(-\frac{r_1^2 + r_2^2}{\rho_0^2}\right). \quad (\text{A1})$$

By means of the equation [9]

$$\int_0^{2\pi} \exp[-in\varphi_1 + i\eta \cos(\varphi_1 - \varphi_2)] d\varphi_1 = 2\pi \exp(-in\varphi_2) I_n(\eta), \quad (\text{A2})$$

where $I_n(\cdot)$ is the modified Bessel function of the first kind with order n , the p order part of $P(\xi|\xi, p_0)$ can be expanded as

$$P(\xi, p|\xi, p_0) = \int_0^\infty \int_0^\infty (a^4 s_0^{n,n,n,n} + b^4 s_0^{m,m,m,m} + a^2 b^2 s_0^{n,m,m,n} + a^2 b^2 s_0^{m,n,n,m} + a^2 b^2 s_{n-m}^{m,m,n,n} + a^2 b^2 s_{m-n}^{n,n,m,m}) \times r_1 r_2 dr_1 dr_2. \quad (\text{A3})$$

The probability of an OAM eigenstate $|l_2, p_0\rangle$ turning into another one $|l_1, p\rangle$ can be expressed as [24]

$$P(l_1, p|l_2, p_0) = \int_0^\infty \int_0^\infty s_{l_2-l_1}^{l_1, l_1, l_2, l_2} r_1 r_2 dr_1 dr_2. \quad (\text{A4})$$

Here we denote that

$$F_{p_0}^p = \int_0^\infty \int_0^\infty (a^4 s_0^{n,n,n,n} + b^4 s_0^{m,m,m,m} + a^2 b^2 s_0^{n,m,n,m} + a^2 b^2 s_0^{m,n,m,n}) r_1 r_2 dr_1 dr_2, \quad (\text{A5})$$

$$R_{p_0}^p = a^2 b^2 [P(n, p|m, p_0) + P(m, p|n, p_0)], \quad (\text{A6})$$

then $P(\xi, p|\xi, p_0)$ can be expressed as

$$P(\xi, p|\xi, p_0) = F_{p_0}^p + R_{p_0}^p. \quad (\text{A7})$$

REFERENCES

- [1] H. Huang, G. D. Xie, Y. Yan, N. Ahmed, Y. X. Ren, Y. Yue, D. Rogawski, M. J. Willner, B. I. Erkmen, K. M. Birnbaum, S. J. Dolinar, M. P. J. Lavery, M. J. Padgett, M. Tur, and A. E. Willner, "100 Tbit/s free-space data link enabled by three-dimensional multiplexing of orbital angular momentum, polarization, and wavelength," *Opt. Lett.*, vol. 39, no. 2, pp. 197–200, 2014.
- [2] M. Mirhosseini, O. S. Magana-Loaiza, M. N. O'Sullivan, B. Rodenburg, M. Malik, M. P. J. Lavery, M. J. Padgett, D. J. Gauthier, and R. W. Boyd, "High-dimensional quantum cryptography with twisted light," *New J. Phys.*, vol. 17, pp. 033033, 2015.
- [3] S. C. Mi, T. J. Wang, G. S. Jin, and C. Wang, "High-Capacity Quantum Secure Direct Communication With Orbital Angular Momentum of Photons," *IEEE Photonics J.*, vol. 7, pp. 7600108, 2015.
- [4] A. Z. Khoury, and P. Milman, "Quantum teleportation in the spin-orbit variables of photon pairs," *Phys. Rev. A*, vol. 83, pp. 060301(R), 2011.
- [5] G. Gibson, J. Courtial, M. J. Padgett, M. Vasnetsov, V. Pas'ko, S. M. Barnett, and S. Franke-Arnold, "Free-space information transfer using light beams carrying orbital angular momentum," *Opt. Express*, vol. 12, no. 22, pp. 5448–5456, 2004.
- [6] R. Celechovsky, and Z. Bouchal, "Optical implementation of the vortex information channel," *New J. Phys.*, vol. 9, pp. 328, 2007.
- [7] Z. X. Wang, N. Zhang, and X. C. Yuan, "High-volume optical vortex multiplexing and de-multiplexing for free-space optical communication," *Opt. Express*, vol. 19, no. 2, pp. 482–492, 2011.
- [8] C. Paterson, "Atmospheric Turbulence and Orbital Angular Momentum of Single Photons for Optical Communication," *Phys. Rev. Lett.*, vol. 94, pp. 153901, 2005.
- [9] Y. Zhu, L. C. Zhang, Z. D. Hu, and Y. X. Zhang, "Effects of non-Kolmogorov turbulence on the spiral spectrum of Hypergeometric-Gaussian laser beams," *Opt. Express*, vol. 23, no. 7, pp. 9137–9146, 2015.
- [10] Y. X. Zhang, M. J. Cheng, Y. Zhu, J. Gao, W. Y. Dan, Z. D. Hu, and F. S. Zhao, "Influence of atmospheric turbulence on the transmission of orbital angular momentum for Whittaker-Gaussian laser beams," *Opt. Express*, vol. 22, no. 18, pp. 22101–22110, 2014.
- [11] Jaime A. Anguita, Mark A. Neifeld, and Bane V. Vasic, "Turbulence-induced channel crosstalk in an orbital angular momentum-multiplexed free-space optical link," *Opt. Appl.*, vol. 47, no. 13, pp. 2414–2429, 2008.
- [12] J. R. Kerr, "Experiments on Turbulence Characteristics and Multiwavelength Scintillation Phenomena," *J. Opt. Soc. Am.*, vol. 62, no. 9, pp. 1040–1049, 1972.
- [13] L. Torner, J. P. Torres, and S. Carrasco, "Digital spiral imaging," *Opt. Express*, vol. 13, no. 3, pp. 873–881, 2005.
- [14] Y. X. Zhang, Y. G. Wang, J. C. Xu, J. Y. Wang, and J. J. Jia, "Orbital angular momentum crosstalk of single photons propagation in a slant non-Kolmogorov turbulence channel," *Opt. Commun.*, vol. 284, pp. 11321138, 2011.
- [15] L. X. Chen, and J. Romero, "Hardys nonlocality proof using twisted photons," *Opt. Express*, vol. 20, no. 19, pp. 21687–21692, 2012.
- [16] J. Romero, J. Leach, B. Jack, S. M. Barnett, M. J. Padgett, and S. Franke-Arnold, "Violation of Leggett inequalities in orbital angular momentum subspaces," *New J. Phys.*, vol. 12, pp. 123007, 2010.
- [17] H. Haken, *Synergetics. An introduction. Nonequilibrium phase transitions and self-organization in physics, chemistry and biology*, New York: Springer-Verlag, 1977.
- [18] J. P. Torres, Y. Deyanova, L. Torner, and G. Molina-Terriza, "Preparation of engineered two-photon entangled states for multidimensional quantum information," *Phys. Rev. A*, vol. 67, pp. 052313, 2003.
- [19] M. J. Cheng, Y. X. Zhang, Y. Zhu, J. Gao, W. Y. Dan, Z. D. Hu, and F. S. Zhao, "Effects of non-Kolmogorov turbulence on the orbital angular momentum of HankelBesselSchell beams," *Opt. Laser Technol.*, vol. 67, pp. 20–24, 2015.
- [20] C. H. Rao, W. H. Jiang, and N. Ling, "Spatial and temporal characterization of phase fluctuations in non-Kolmogorov atmospheric turbulence," *J. Mod. Opt.*, vol. 47, no. 6, pp. 1111–1126, 2000.
- [21] Y. D. Liu, C. Q. Gao, and M. W. Gao, "Study on holographic grating diffraction for Laguerre Gaussian beam generation," *Chin. Phys. B*, vol. 17, no. 5, pp. 1769–1776, 2008.
- [22] N. Uribe-Patarroyo, A. Alvarez-Herrero, and T. Belenguer, "Measurement of the quantum superposition state of an imaging ensemble of photons prepared in orbital angular momentum states using a phase-diversity method," *Phys. Rev. A*, vol. 81, pp. 053822, 2010.
- [23] L. X. Chen, W. H. Zhang, Q. H. Lu, and X. Y. Lin, "Making and identifying optical superpositions of high orbital angular momenta," *Phys. Rev. A*, vol. 88, pp. 053831, 2013.
- [24] D. Giovannini, E. Nagali, L. Marrucci, and F. Sciarrino, "Resilience of orbital-angular-momentum photonic qubits and effects on hybrid entanglement," *Phys. Rev. A*, vol. 83, pp. 042338, 2011.